IJNAOE
©SNAK, 2014

Int. J. Nav. Archit. Ocean Eng. (2014) 6:947~964
http://dx.doi.org/10.2478/IJNAOE-2013-0224
pISSN: 2092-6782, eISSN: 2092-6790

Effects of vertical wall and tetrapod weights on wave overtopping in rubble mound breakwaters under irregular wave conditions

Sang Kil Park[1], Asgar Ahadpour Dodaran[2], Chong Soo Han[2] and Mohammad Ebrahim Meshkati Shahmirzadi[3]

[1]*Department of Civil Engineering, Pusan National University, Busan, South Korea*
[2]*Department of Civil Engineering, Pusan National University, Busan, South Korea*
[3]*Post-docotoral researcher, Disaster Prevention Research Institute, Kyoto University, Kyoto, Japan*

ABSTRACT: *Rubble mound breakwaters protect the coastal line against severe erosion caused by wave action. This study examined the performance of different sizes and properties (i.e. height of vertical wall and tetrapod size) of rubble mound breakwaters on reducing the overtopping discharge. The physical model used in this study was derived based on an actual rubble mound in Busan Yacht Harbor. This research attempts to fill the gap in practical knowledge on the combined effect of the armor roughness and vertical wall on wave overtopping in rubble mound breakwaters. The main governing parameters used in this study were the vertical wall height, variation of the tetrapod weights, initial water level elevation, and the volume of overtopping under constant wave properties. The experimental results showed that the roughness factor differed according to the tetrapod size. Furthermore, the overtopping discharge with no vertical wall was similar to that with relatively short vertical walls ($\gamma_v = 1$). Therefore, the experimental results highlight the importance of the height of the vertical wall in reducing overtopping discharge. Moreover, a large tetrapod size may allow coastal engineers to choose a shorter vertical wall to save cost, while obtaining better performance.*

INTRODUCTION

The rubble mound breakwater is one of the most common breakwater types used for shore protection, which involves several tetrapod layers. One of the greatest influences on the design of a breakwater is the overtopping hydraulic procedure. The overtopping manual provides management guidelines on the analysis and estimation of the overtopping discharge volume to control flooding when breakwaters are subject to significant wave action. On the other hand, there has been little research on the role of the overtopping parameter in design. A few overtopping studies have been reported for seawalls (Owen, 1980; Goda, 1985), and more recently for rubble mound breakwaters (Aminti and Franco, 1988; Bradbury and Allsop, 1988; Goda, 1985). An extensive study was published by Van der Meer and De Waal (1993). Franco et al. (1994) established a formula for the overtopping discharge volume of vertical breakwaters. Franco (1993) also evaluated the effect of overtopping volumes on persons and cars behind the crown wall of a vertical breakwater. Saville and Caldwell (1953) researched the wave overtopping volumes and wave run-up height, whereas (Jensen and JuhI, 1987; Weggel, 1976; Van der Meer, 2002) analyzed the data of previous studies**.** Several formulae can be used to estimate the mean overtopping discharge at toe structures. On the other hand, it was not the aim of this study to calculate these formulae, rather, this study focused on the roughness influence factor, which

Corresponding author: *Asgar Ahadpour Dodaran*, e-mail: *asgar.ahadpour2@pusan.ac.kr*

can also be applied to wave overtopping estimations by Van der Meer (2002). On wave overtopping, previous studies tried to separate out these influences, but the findings were inconclusive Franco et al. (2009). The overtopping performance of different armor units for rubble mound breakwaters and the roughness influence factor was investigated experimentally by Bruce et al. (2009) but only a single tetrapod size was considered. The port of Busan is a vital gateway in Korea, connecting the country to the Pacific Ocean and Asia. This port is Korea's main port, handling approximately 40% of the country's overseas cargo, 80% of its container cargo, and 40% of Korea's national fishery production. Breaking waves play an important role in almost all coastal engineering issues Busan Port Authority (2011). A key function of breakwaters is to provide protection against waves in harbors and nearby channels, as well as currents and siltation. In South Korea's Busan Yacht Harbor (Fig. 1), breakwater rubble mounds have been studied. Rubble mound breakwaters in this area of the beach are the most suitable structures for this investigation, which were designed to test irregular waves. The hydraulic responses of a breakwater are one of the most significant factors for the design of rubble mounds. Another major factor for embedding the breakwater is the overtopping-related issue.

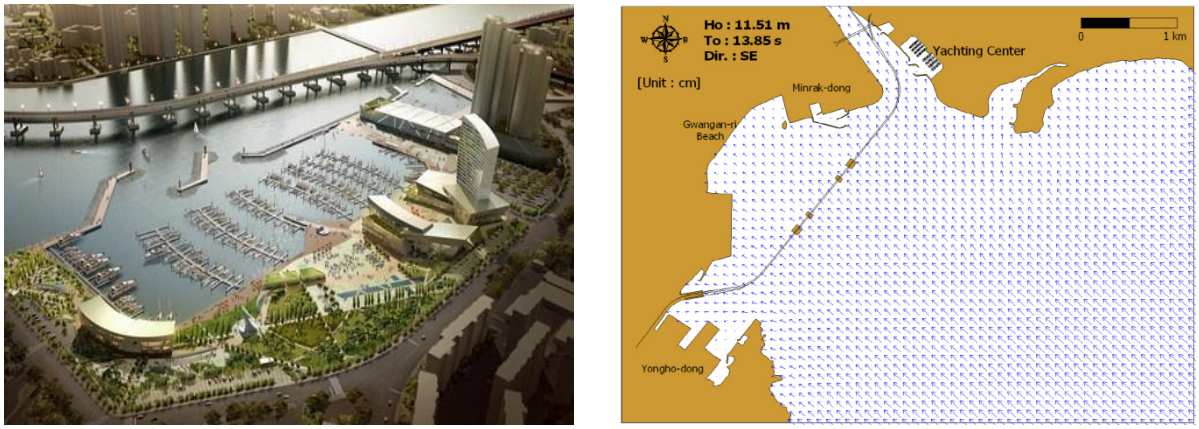

Fig. 1 Yacht harbor position, busan, south korea.

Pullen et al. (2007) suggested the installation of vertical walls on the rubble mound breakwater structure to reduce the overtopping discharge. They recommended that the vertical wall not be much higher than the armor crest level because wave forces on the wall will increase drastically if attacked directly by waves and not hidden behind the armor crest Pullen et al. (2007).

Model set-up

An extensive number of experimental tests in the wave flume located at coastal engineering research institute, Pusan National University, Busan, South Korea were conducted to achieve the main purposes of this study. The wave flume used in this study was a 30 *m* long rectangular channel with a transparent Plexiglas sidewall. The width and height of this flume were 0.6 *m* and 1.0 *m*, respectively. A foreshore with a front slope of 1:30 was constructed in the flume. The beginning of the foreshore was located 22.5 *m* far downstream from the wave generators. Fig. 2 presents a schematic (not to scale) view of the rubble mound physical model.

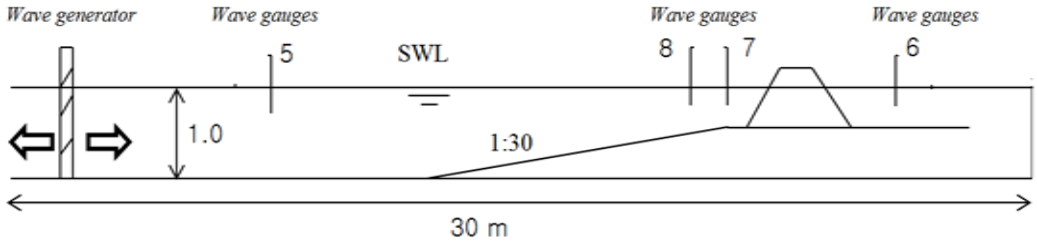

Fig. 2 Experimental setup.

A 0 degree wave generator paddle, which was controlled by a computer program, was used to mechanically provide irregular waves in the flume. Using the computer program, the wave properties (wave period & wave height) were controlled; with concern to the scale factor between the physical model and actual case study. To measure the variation in the wave properties, 4 wave gauges were placed along the flume. The first wave gauge was positioned in front of the wave generator called Channel 5, which is the target wave height of the rubble mound breakwater in the Busan Yacht Harbour model. The second wave gauge was 2.0 *m* upstream from the crest of the rubble mound structure called Channel 8. The third gauge was located 1.0 *m* upstream from the crest of the rubble mound structure and was called Channel 7. The last gauge (Channel 6) was positioned behind the structure at a 1 m distance from the crest in the rubble mound (Fig. 2). tetrapods of different sizes and weights, namely 8 *ton*, 12 *ton*, 16 *ton*, and 20 *ton*, were considered. Fig. 3 shows a photograph of the different tetrapods used in the present study. Table 1 compares the weights of the tetrapods between the actual and physical model. The distance from the crest height of the tetrapod to the superstructure was constant for all test conditions. Four initial water level elevations were examined, which are defined in Table 2.

Fig. 3 Photograph of the tetrapods used in the present study.

Table 1 Comparison of weight of the tetrapods in the actual and physical model.

Tetrapod size	Prototype (*ton*)	Model (*g*)
8*ton*	7.36	115
12*ton*	11.50	179
16*ton*	14.49	226
20*ton*	18.40	287

Table 2 Four different water levels examined and the corresponding design level (D.L).

Water Level definition	Naming system	Elevation
Storm Surging	S.S	(DL.(±)3.382 *m*)
Height of High Water	H.H.W	(DL.(±)1.282 *m*)
Mean Sea Level	M.S.L	(DL.(+)0.641 *m*)
Lower Low Water	L.L.W	(DL.(+)0.000 *m*)

Experimental procedure

After setting up the structure in the flume, the water inlet valve was opened until the desired water level in the flume was reached Storm Surging (S.S), Height of High Water (H.H.W), Mean Sea Level (M.S.L), and Lower Low Water (L.L.W), and the wave generator system was then started using a personally controlled program for the maximum wave height. The maximum wave height cannot be determined as a definite value, but can be expressed as the most probable maximum value for a given number of waves *N* using equation 1:

$$\frac{H_{\max}}{H_{1/3}} \approx \frac{1}{1.416}\left[\left(\ln N\right)^{0.5} + \frac{\gamma}{2}\left(\ln N\right)^{-0.5}\right] \approx 1.07\sqrt{\log_{10} N} \text{ (for large } N\text{)} \quad (1)$$

Table 3 lists the values calculated using Eq. (1), in which $\gamma = 0.5772$.

Table 3 Ratio in N waves of $H_{\max}$ to $H_{1/3}$.

N	50	100	200	500	1000	10000
$H_{\max} / H_{1/3}$	1.42	1.53	1.64	1.77	1.86	2.15

The ratio in N waves of $H_{\max}$ to $H_{1/3}$ in this study was 1.86, because 1000 waves were generated.

$$H_{\max} = 1.86 \times (\text{scale=1/40}) \times 4.6m\left(H_{1/3}\right) = 21.4cm$$

where $H_{\max}$ is the maximum wave height in the computer program capable of starting the wave generator in the physical model, scale is the 1/40 physical model used in the laboratory, and $H_{1/3}$ is the significant wave height of the prototype model. After starting the experiment, the duration of the tests was fixed to 30 minutes for each of the four water levels time series of 30 minutes each, and each gauge's location in the flume was saved on a computer. For overtopping discharge volume analysis and the creation of the energy spectrum, 2000 data points were used.

Measurement device

Two gauges were positioned seaward (Channel 7 and 8) of the rubble mound structure. The incident and reflected conditions were separated using the Pusan National University WaveLab software, as described by Mansard and Funke (1980). The wave surface elevation at any location and time (t) can be expressed as follows (Fig. 4).

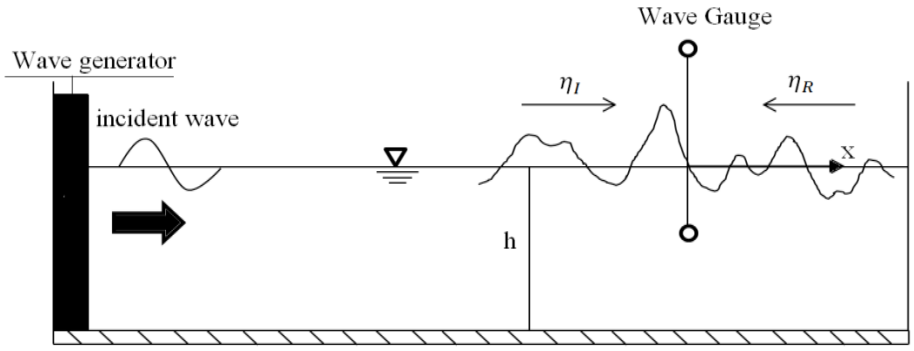

Fig. 4 Sketch of a wave flume using a one wave gauge.

$$\eta(t) = \eta_I(t) + \eta_R(t) \quad (2)$$

$$\eta(t) = \frac{H_i}{2}\cos(kx - \sigma t) + \frac{H_r}{2}\cos(kx + \sigma t + \varepsilon) \quad (3)$$

where η_I and η_R are the surface elevations of incident and reflected waves, H_i is the wave height for the incident wave, H_r is the wave height for the reflected wave, ε is an error due to signal noise, σ is the angular frequency, and k is the wave number of $2\pi / L$ with L being the wavelength because

$$\left.\begin{aligned}\cos(a-b)&=\cos a\cos b+\sin a\sin b\\ \cos(a+b)&=\cos a\cos b-\sin a\sin b\end{aligned}\right\} \tag{4}$$

Substituting Eq. (4) into Eq. (3) yields:

$$\begin{aligned}\eta&=\left[\frac{H_i}{2}\left(\cos kx\cos\alpha t+\sin kx\sin\sigma t\right)+\frac{H_r}{2}\left(\cos(kx+\varepsilon)\cos\sigma t-\sin(kx+\varepsilon)\sin\sigma t\right)\right]\\ &=\left[\frac{H_i}{2}\cos kx+\frac{H_r}{2}\cos(kx+\varepsilon)\right]\cos\sigma t+\left[\frac{H_i}{2}\sin kx-\frac{H_r}{2}\sin(kx+\varepsilon)\right]\sin\sigma t\end{aligned}$$

$$\eta(t)=I(x)\cos\sigma t+F(x)\sin\sigma t \tag{5}$$

The water level to obtain the maximum point in Eq. (5), $\frac{\partial\eta(x_m,t_m)}{\partial t}=0$ can be expressed as

$$\frac{\partial\eta(t)}{\partial t}=-I(x)\sigma\sin\sigma t+F(x)\sigma\cos\sigma t=0$$

$$\tan(\sigma t)_{\max}=\frac{F(x)}{I(x)} \tag{6}$$

Substituting Eq. (6) into Eq. (5) yields:

$$\eta(t)_{peak}=\frac{I(x)^2+F(x)^2}{\sqrt{I(x)^2+F(x)^2}}=\pm\sqrt{I(x)^2+F(x)^2} \tag{7}$$

Finally, the above procedures gave $\eta(t)_{\min}$ and $\eta(t)_{\max}$, which after solving the equation, the incident wave and reflected wave heights can be calculated as follows:

$$H_i=\eta(t)_{\max}+\eta(t)_{\min} \tag{8}$$

$$H_r=\eta(t)_{\max}-\eta(t)_{\min} \tag{9}$$

In the entire test series, the target incident wave height was 20.70 *cm*. This incident wave height is close to the limit of capacity of the wave generator (Fig. 5) in the laboratory, Pusan National University, Busan, South Korea. Therefore, the measured wave heights are predicted to be slightly lower than 21.40 *cm*.

The wave heights were measured and calculated using the time history data. Fig. 5 shows the time history of the water surface for wave gauges No. 5~8. The maximum amplitude above the still water level was approximately +11 *cm* and it appears that the amplitude could not exceed the certain limit (11 *cm*), while the amplitude below the still water level was a maximum (-10 *cm*).

A Bretschneider Mitsuyasu spectrum was produced with $H_i=11.5\ \ cm$ being a significant wave height and $T_i=2.53s$ a significant wave period. These were measured using gauges at the specific locations mentioned above. Table 1 lists the four water depths (S.S, H.H.W, M.S.L, L.L.W) of the model. An input file has to be created by the user, stipulating the requested wave height, wave period, wave spectrum, spectrum parameters, and duration.

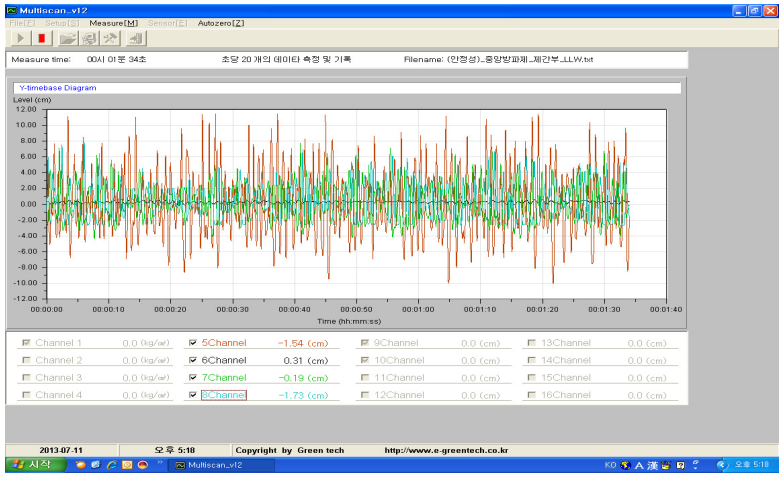

Fig. 5 Instantaneous free surface elevation time series in the H.H.W water level.

This experiment used a double layer of 20 *ton*, 16 *ton*, 12 *ton* and 8 *ton* tetrapods in two colour combinations (blue and yellow, red and green), as shown in Fig. 2. In the computer program, the wave height was adjusted to 20.7 *cm* when the wave generator was used in the physical model test. The Bretschneider–Mitsuyasu spectrum was used for the experimental output to realize the capacity of the energy spectrum for different locations of the flume (in front of and behind the structure). The Bretschneider–Mitsuyasu spectrum was set by:

$$S(f) = 0.205\left(H_{1/3}\right)^2 \times \left(T_{1/3}\right)^{-4} \times f^{-5} \exp\left(-0.75 \times \left(T_{1/3} \times f^{-4}\right)\right) \times 0.0001 \tag{10}$$

where $S(f)$ is the energy spectrum according to the Bretschneider–Mitsuyasu spectrum method, f is the frequency that obtained the wave period, $H_{1/3}$ is the significant wave height and $T_{1/3}$ is the significant wave period, as shown in Table 4.

Table 4 Data of the rubble mound breakwater.

Water level	Double layer tetrapod (*ton*)	$H_{1/3}\,(cm)$ (1)	$T_{1/3}\,(s)$ (1)	$H_{1/3}\,(cm)$ (2)	$T_{1/3}\,(s)$ (2)	$H_{1/3}\,(cm)$ (3)	$T_{1/3}\,(s)$ (3)
S.S	20	10.85	1.25	10.80	1.26	10.86	1.27
	16	11.21	1.82	11.10	1.82	11.32	1.80
	12	11.34	1.52	11.22	1.51	11.28	1.51
	8	11.85	1.51	11.74	1.50	11.86	1.51
H.H.W	20	10.76	1.24	10.68	1.25	10.80	1.22
	16	10.98	1.76	10.91	1.74	10.95	1.75
	12	11.25	1.44	11.23	1.41	11.26	1.44
	8	11.36	1.42	11.21	1.45	11.30	1.42
M.S.L	20	9.39	1.22	9.31	1.23	9.38	1.21
	16	9.56	1.67	9.46	1.65	9.57	1.68
	12	9.86	1.65	9.82	1.64	9.88	1.66
	8	10.2	1.40	10.27	1.42	10.20	1.42
L.L.W	20	8.36	1.15	8.31	1.16	8.40	1.32
	16	8.42	2.79	8.40	2.82	8.42	2.59
	12	8.56	1.29	8.56	1.31	8.60	1.39
	8	8.63	1.29	8.60	1.27	8.601	1.19

Test configuration

In this experiment, several mixtures of the freeboard crest height and wave steepness were created to obtain the overtopping discharge (Table 5).

Where H_i is the significant wave height at toe, s_{om} is the wave steepness, and R_c is the free crest height (freeboard).

Table 5 Variation of the parameters.

Series	H_i (cm)	s_{om}	Armor units (ton)	R_c (cm)
Case1	8.0, 11.0, 13.0	0.02, 0.04, 0.06	8, 12, 16, 20	1.0, 6.22, 7.82, 9.43
Case2	8.0, 11.0, 13.0	0.02, 0.04, 0.06	8, 12, 16, 20	2.75, 8.0, 9.60, 11.20
Case3	8.0, 11.0, 13.0	0.02, 0.04, 0.06	8, 12, 16, 20	4.80, 10.0, 11.65,13.25
Case4	8.0, 11.0, 13.0	0.02, 0.04, 0.06	8, 12, 16, 20	7.80, 13.0, 14.60,16.25
Case5	8.0, 11.0, 13.0	0.02, 0.04, 0.06	8, 12, 16, 20	10.30, 15.50, 17.15, 18.75

Definition of overtopping

To determine the validity of the results for overtopping in this research, the current data was compared with the Van der Meer (2002) formula, which describes the overtopping discharge for irregular waves. A comparison of the results of this experiment with Van der Meer's formula, showed that the present overtopping discharge estimator provides good results.

Two formulae for the average wave overtopping in the case of irregular waves have been described Van der Meer (2002). The combination of the rubble mound structure slope and wave steepness gives an estimation of a breaking wave. $\xi = \frac{\tan\alpha}{\sqrt{s_{om}}}$, where ξ_{om} is the breaker parameter and α is the slope of the front of the rubble mound structure. When $\gamma_m \xi_{om} > 2$, non-breaking waves are present, whereas for $\gamma_b \xi_{om} \le 2$, breaking waves are present. The complete formula (Van der Meer, 2002; Pullen et al., 2007) is

$$\frac{q}{\sqrt{gH_i^3}} = \frac{0.067}{\sqrt{\tan\alpha}} \gamma_b \xi_{om} \exp\left(-4.7 \frac{R_c}{H_i \xi_{om} \gamma_b \gamma_f \gamma_\beta \gamma_v} \right) \tag{11}$$

where q is the overtopping discharge ($m^3/m/s$), H_i is the significant wave height at the toe of the rubble mound breakwater (m), g is the gravitational acceleration (m/s^2), γ_f is the influence factors of roughness(γ_f), γ_β is the influence factors of the angle of wave attack ($\gamma_\beta = 1$), γ_b is the influence factors for the effects of the toe of the breakwater, γ_v is the influence factors for the effects of the foreland (γ_v), and ξ_{om} is the breaker parameter, which this study checked in the breaking wave condition.

Van der Meer's (2002) formula in the breaking condition with a maximum of ($\gamma_b \xi_{om} = 2$) can be described as

$$\frac{q}{\sqrt{gH_i^3}} = 0.2 \exp\left(-2.6 \frac{R_c}{H_i \gamma_f \gamma_\beta} \right) \tag{12}$$

Influence factor for roughness (γ_f)

The results of this experiment were compared with those of Van der Meer (2002). As shown in Fig. 6, the experimental results of the effect of the roughness factor are consistent with Van der Meer (2002). Van der Meer (2002) suggested that if R_c equals A_c, the maximum overtopping is as follows in Eq. (12).

Furthermore, if gamma γ_β equals 1 (Eq. (13)):

$$\frac{q}{\sqrt{gH_i^3}} = 0.2\exp\left(-2.6\frac{R_c}{H_i\gamma_f}\right) \tag{13}$$

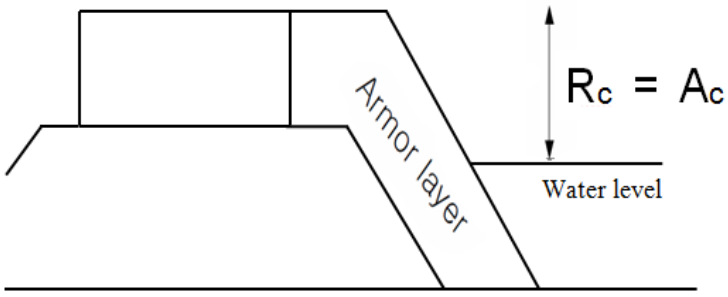

Fig. 6 Freeboard level and location for wave overtopping ($R_c = A_c$), Case 1.

Influence factor for a vertical wall (γ_v)

First, the roughness factor was obtained for each tetrapod size in presence of no vertical walls. By assuming that the roughness factor is constant, this study examined the influence of different vertical walls on the overtopping discharge (Eq. (14)).

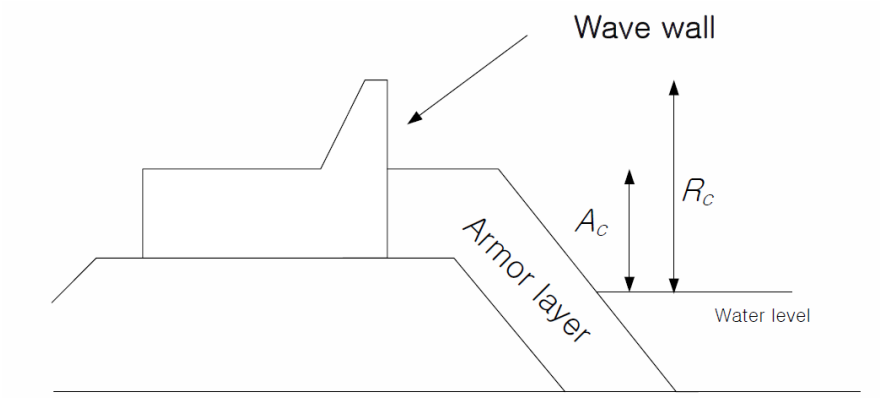

Fig. 7 Freeboard level and location for wave overtopping (Case 2, 3, 4 and 5).

$$\frac{q}{\sqrt{gH_i^3}} = \frac{0.067}{\sqrt{\tan\alpha}}\gamma_b\xi_{om}\exp\left(-4.75\frac{R_c}{H_i\xi_{om}\gamma_\beta\gamma_v}\right) \tag{14}$$

Results and discussion

Wave Spectrum

In the case of each water level (S.S, H.H.W, M.S.L, and L.L.W), the increase in frequency raised the energy spectrum. The energy spectrum is strongly related to the significant wave, $H_{1/3}$. On Channel 5, the significant wave height is higher than that at the other locations of the gauges (Channels 6, 7 and 8). Therefore, the energy spectrum on Channel 5 is much

higher and stronger than at the other gauges' positions (Fig. 8).

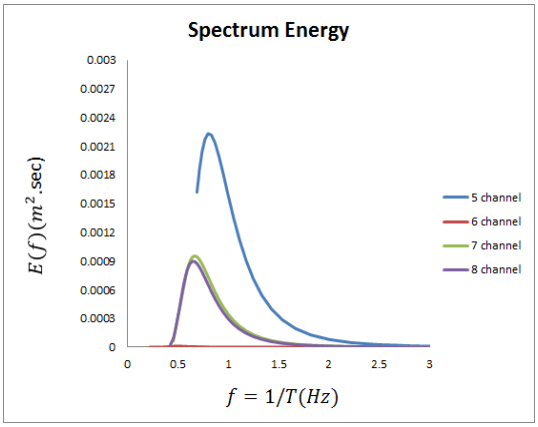

(a) Bretschneider–Mitsuyasu spectrum (S.S).

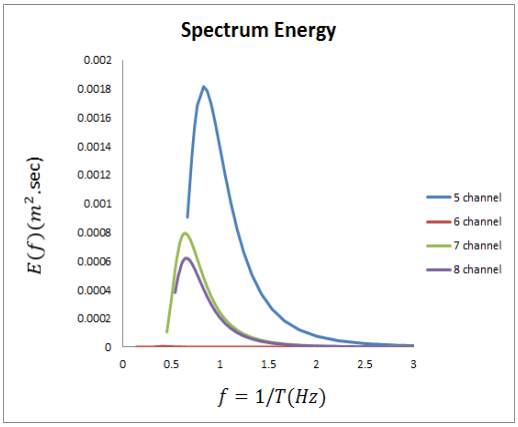

(b) Bretschneider–Mitsuyasu spectrum (H.H.W).

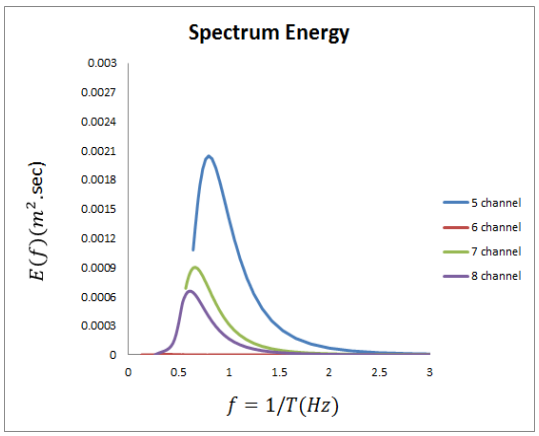

(c) Bretschneider–Mitsuyasu spectrum (M.S.L).

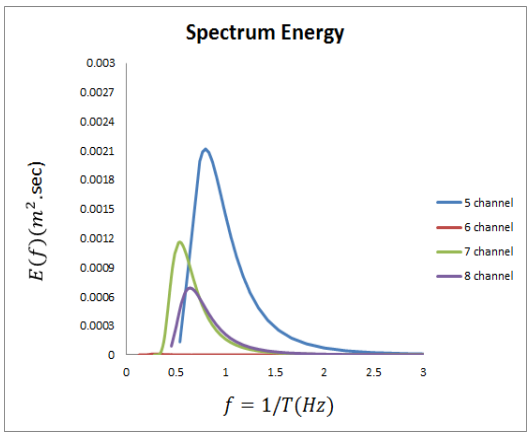

(d) Bretschneider–Mitsuyasu spectrum (L.L.W).

Fig. 8 Illustration of the wave spectrum at the four water levels (a, b, c and d), Case 1.

The wave heights decrease at wave gauges No 7 and 8 compared to No 5. The wave height would otherwise increase or amplify due to the shoaling effect by the bottom slope without wave breaking. A comparison of the maximum energy spectrum between the four locations during the storm surging water level revealed the $S(f)$ of Channels 5, 6, 7, and 8 to be 0.0022 $m^2.s$, 0.000015 $m^2.s$, 0.0011 $m^2.s$, and 0.0012 $m^2.s$, respectively. These results mean that when making specific waves using the wave generator, these waves decrease with distance from the generator, so that the significant wave and energy spectrum also decreased. The entire spectrum in Fig. 8 was calculated using the significant wave height, $H_{1/3}$ and $T_{1/3}$, with the Bretschneider–Mitsuyasu spectrum (B-M). Fig. 8 shows that in the case of Channel 6, there was a minimum energy when using the Bretschneider–Mitsuyasu spectrum and it was more meaningful to calculate the spectra directly from the measured wave profiles, because that gauge was located behind the structure and there was very little variation of wave significance.

Time series

Fig. 9 shows the time series of each experiment, describing the surface elevation of the sea state over time. Fig. 9 shows that the elevation of the wave height changed with increasing time and depending on the location of the gauges.

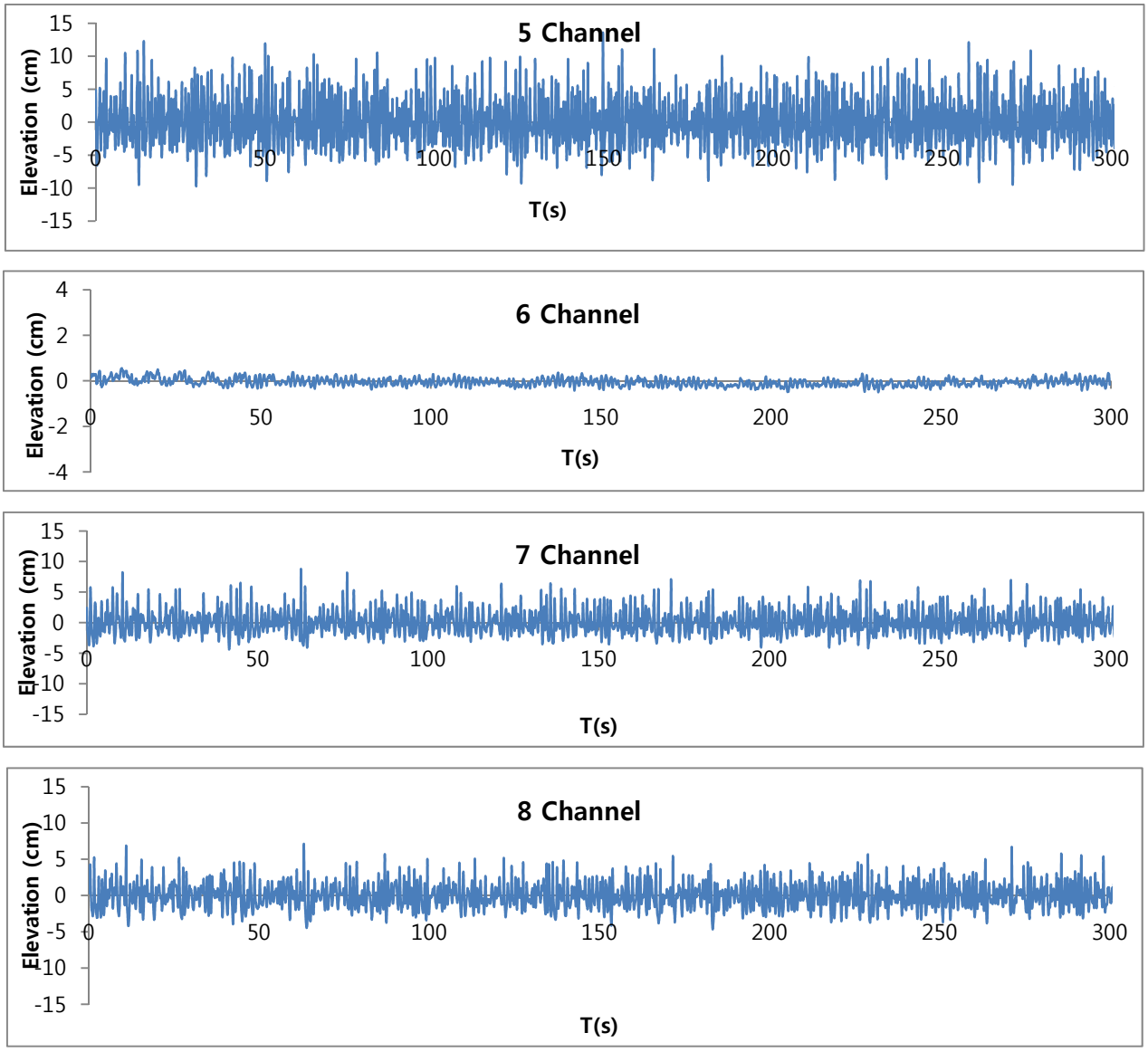

Fig. 9 Time series in the storm surging water level, Case 1.

Case 1: Influence factor for roughness (γ_f), (DL+3.77)

Fig. 10 Case 1 (DL+3.77), no wave wall height.

Each test was carried out under four different initial water levels in the flume and upstream of the rubble mound, namely Low Level of Water (L.L.W), Mean Sea Level (M.S.L), High Water Level (H.W.L), Storm Surging (S.S). As shown in Table 6

and Fig. 10 there was no vertical wall above the crest and R_c equals A_c. Fig. 10 shows the value of the roughness factor for different tetrapods sizes under the no vertical wall condition.

Table 6 Example input file for analysis of the influence factor for a vertical wall (γ_v) with the first 4 calculations.

A_c (cm)	R_c (cm)
1.0	1.0
6.22	6.22
7.82	7.82
9.43	9.43

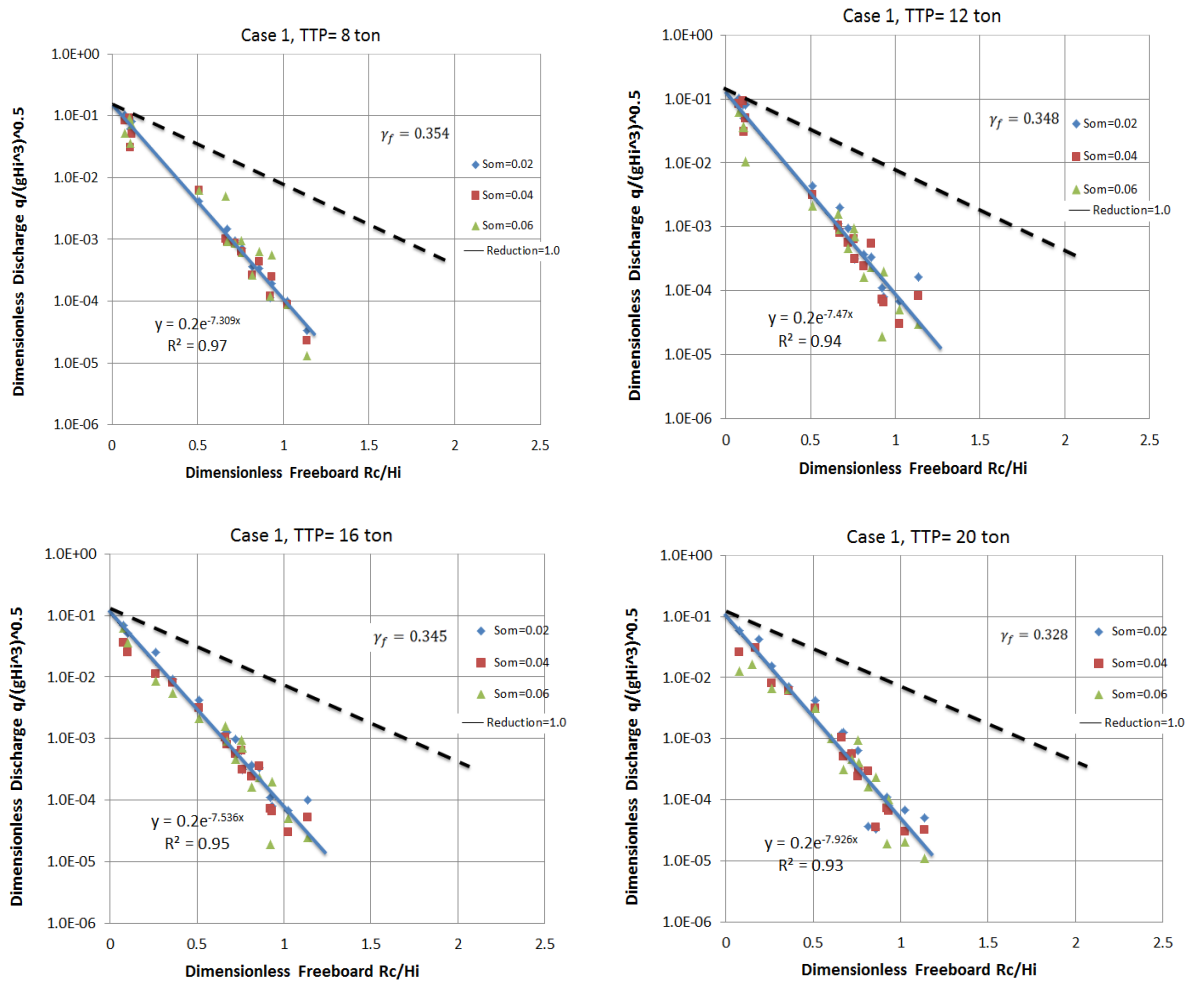

Fig. 11 Graph of the non-dimensional mean overtopping versus dimensionless freeboard for Case 1, TTP = 8 *ton*, 12 *ton*, 16 *ton* and 20 *ton*. The dashed lines are for $\gamma_f = 1.0$.

The test results in this research are given with the common logarithmic displays (Eq. (13)) only in terms of the mean overtopping discharge versus the relative freeboard, and reanalyzed using the technique recommended by Bruce et al. (2009). Using linear regression to determine the roughness factor, γ_f, it is possible to calculate the 95% confidence interval associated with this estimate Bruce et al. (2009). Fig. 11 presents the calculated values of γ_f together with their lower and upper limits. All lines begin at $R_c / H_i = 0$ and $\frac{q}{\sqrt{gH_i^3}} = 0.2$, for smooth slopes $\gamma_f = 1$ and the value for each unit is

derived by fitting a line through the data points. The results obtained by this research were in fair agreement (Fig. 12) with those reported by (Van der Meer, 2002; Bruce et al., 2009). In addition, the overtopping discharge decreased with increasing roughness factor.

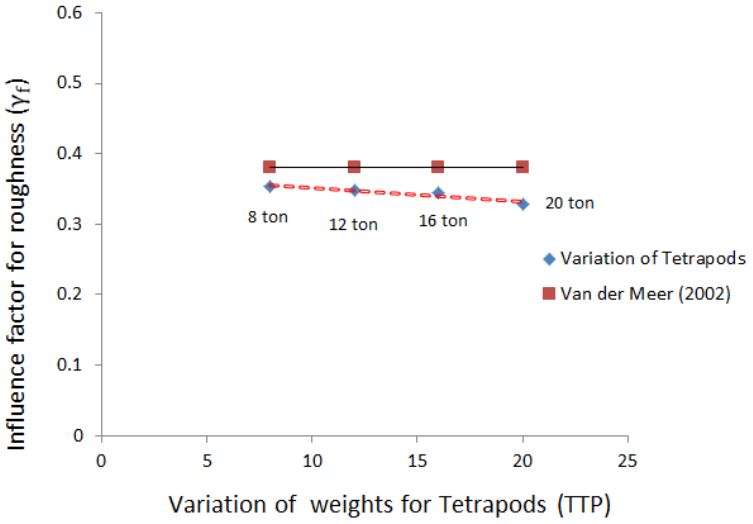

Fig. 12 Calculated values of γ_f together with their lower and upper limits.

Case 2: Influence factor for a vertical wall (γ_v), (DL+4.48)

Fig. 13 Case 2 (DL+4.48), wave wall height (1.78 *cm*).

Four water levels were used (L.L.W, M.S.L, H.H.W, and S.S). Therefore, four Ac and R_c were defined in this study for Case 2 (Table 7).

Table 7 Example input file for an analysis of the influence factor for a vertical wall (γ_v) with first 4 calculations.

A_c (*cm*)	R_c (*cm*)
1.0	2.75
6.22	8.0
7.82	9.60
9.43	11.20

Case 2 refers to those experiments in which the vertical walls are short (Fig. 13). The height of the vertical wall equals the level of the vertical wall crest minus the level of the armor crest, which is equal to 0.71 *m* in the prototype or in other words, 1.78 *cm* in the current physical model with a scale factor of 1/40. This study investigated the effect of different vertical walls on the overtopping discharge assuming that for a given tetrapod size, there is a certain roughness factor regardless of the vertical wall height. The value of the roughness factor for each tetrapod size was measured in Case 1. In Case 2, with a short vertical wall, changing the size of tetrapod did not have a significant effect on the vertical wall roughness (Fig. 14). This means that in presence of short vertical walls, the effect of the roughness factor is more dominant than the effect of the vertical wall factor. On the other hand, the effect of the roughness factor decreases with increasing vertical wall height.

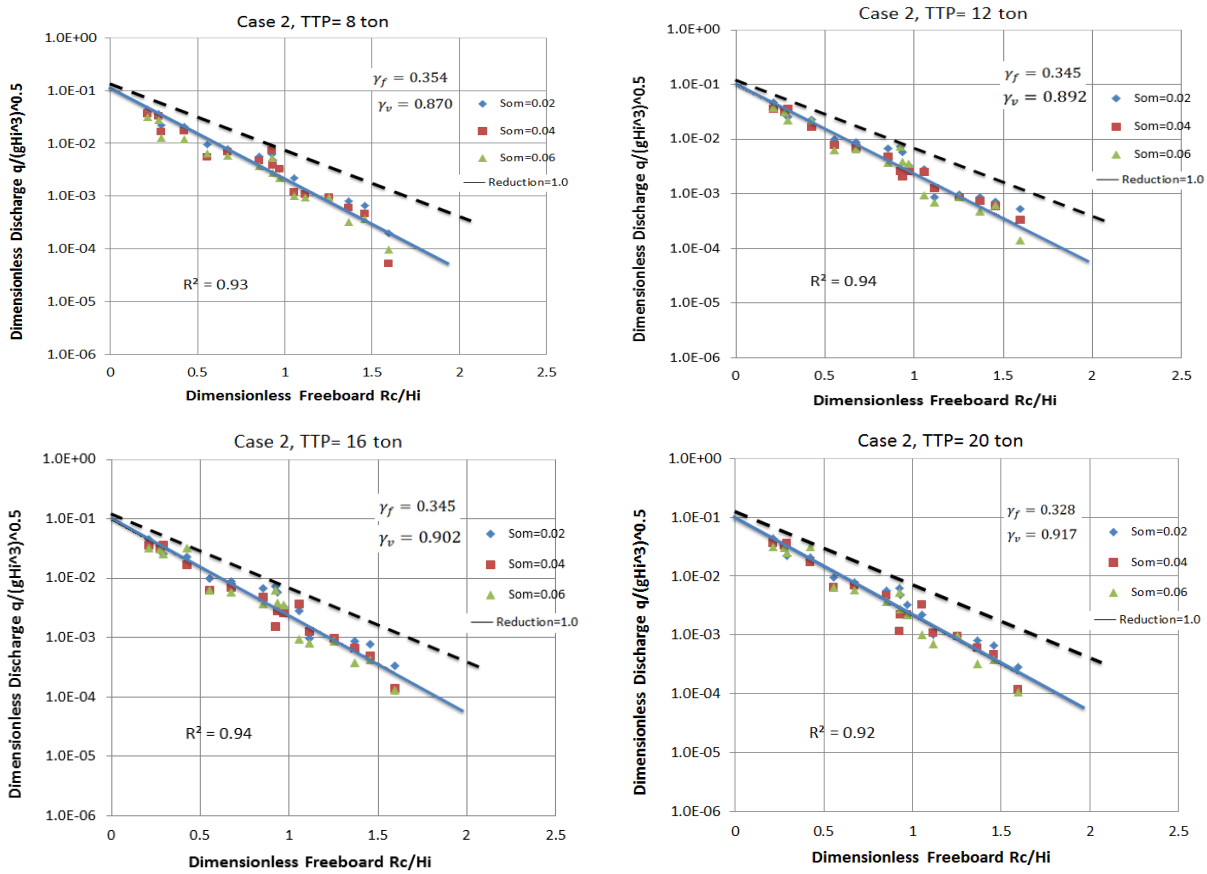

Fig. 14 Graph of non-dimensional mean overtopping versus the dimensionless freeboard for Case 2, TTP = 8 *ton*, 12 *ton*, 16 *ton* and 20 *ton*. The dashed lines are for $\gamma_v = 1.0$

Case 3: Influence factor for a vertical wall (γ_v), (DL+5.30)

Fig. 15 Case 3 (DL+5.30), wave wall height (3.53 *cm*).

Similar to Case 2, four A_c and R_c are defined in this research for Case 3 (Table 8).

Figs. 16, 18 and 20 show the variation of the normalized discharge versus the dimensionless freeboard for Cases 3, 4 and 5, respectively. As shown in Fig. 15, when the vertical wall is taller than 1.78 *cm*, the influence of the vertical wall is more dominant than the effect of the roughness factor. On the other hand, for a given dimensionless discharge and a constant dimensionless freeboard, the effect of the vertical wall on the overtopping discharge decreased with increasing tetrapod size. In other words, choosing a larger tetrapod size would allow a shorter vertical wall that will lead to a more cost effective design. Similar results were obtained in Cases 4 and 5, as shown in Figs. 17 and 19.

Table 8 Example input file for an analysis of the influence factor for a vertical wall (γ_v) with the first 4 calculations.

A_c (cm)	R_c (cm)
1.0	4.80
6.22	10.0
7.82	11.65
9.43	13.25

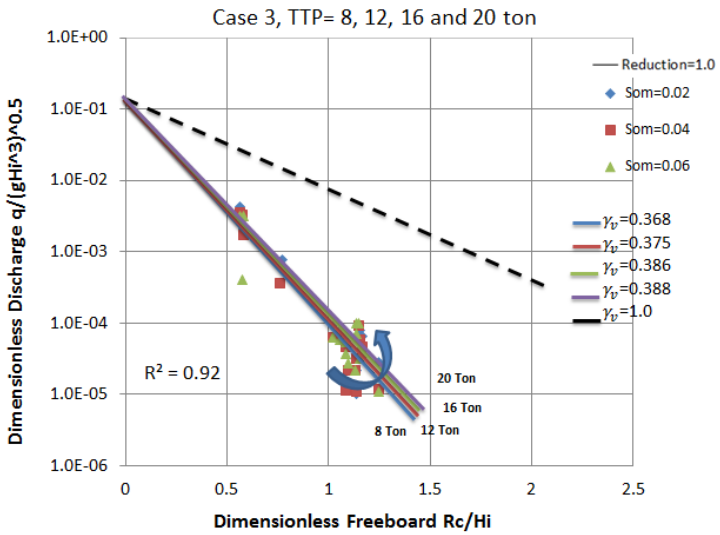

Fig. 16 Graph of non-dimensional mean overtopping versus dimensionless freeboard for Case 3, TTP = 8 *ton*, 12 *ton*, 16 *ton* and 20 *ton*. The dashed lines are for $\gamma_v = 1.0$.

Case 4: Influence factor for a vertical wall (γ_v), (DL+6.50)

Fig. 17 Cass 4 (DL+6.50), wave wall height (6.83 *cm*).

Four Ac and R_c were defined in this research for Case 4 (Table 9) corresponding to the four water levels (L.L.W, MS.L, H.H.W and S.S).

Table 9 Example input file for an analysis of the influence factor for a vertical wall (γ_v) with first 4 calculations.

A_c (cm)	R_c (cm)
1.0	7.80
6.22	13.0
7.82	14.60
9.43	16.25

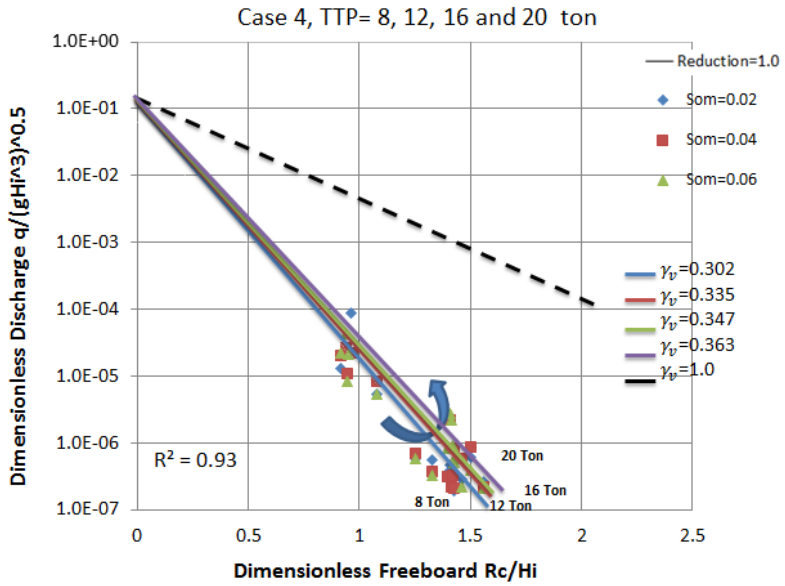

Fig. 18 Graph of non-dimensional mean overtopping versus the dimensionless freeboard for Case 4, TTP = 8 *ton*, 12 *ton*, 16 *ton* and 20 *ton*. The dashed lines are for $\gamma_v = 1.0$.

Case 5: Influence factor for a vertical wall (γ_v)(DL+7.50)

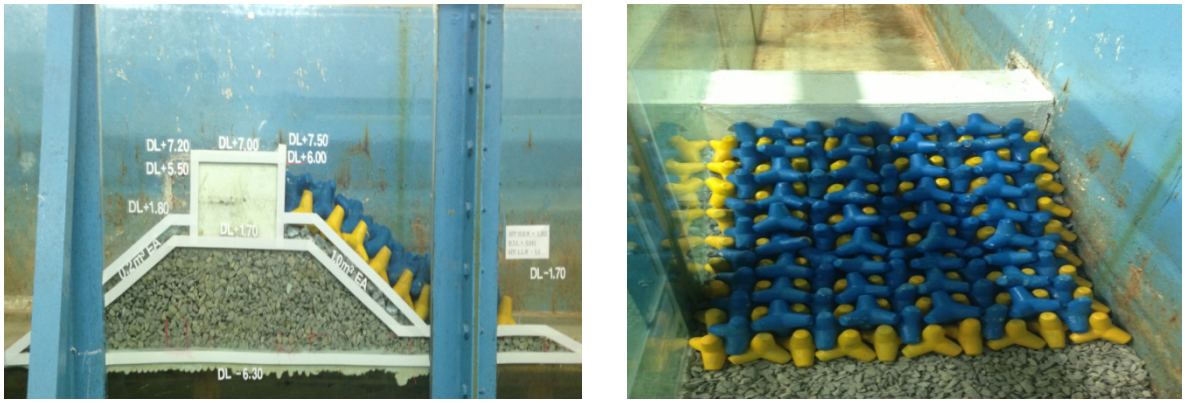

Fig. 18 Case 5 (DL+7.50), wave wall height (9.33 *cm*).

Four water levels (L.L.W, M.S.L, H.H.W, and S.S) were used. Therefore, four A_c and R_c defined in this research for Case 5 (Table 10).

Table 10 Example input file for analysis influence factor for a vertical wall (γ_v) with first 4 calculations.

A_c (cm)	R_c (cm)
1.0	10.30
6.22	15.30
7.82	17.15
9.43	18.75

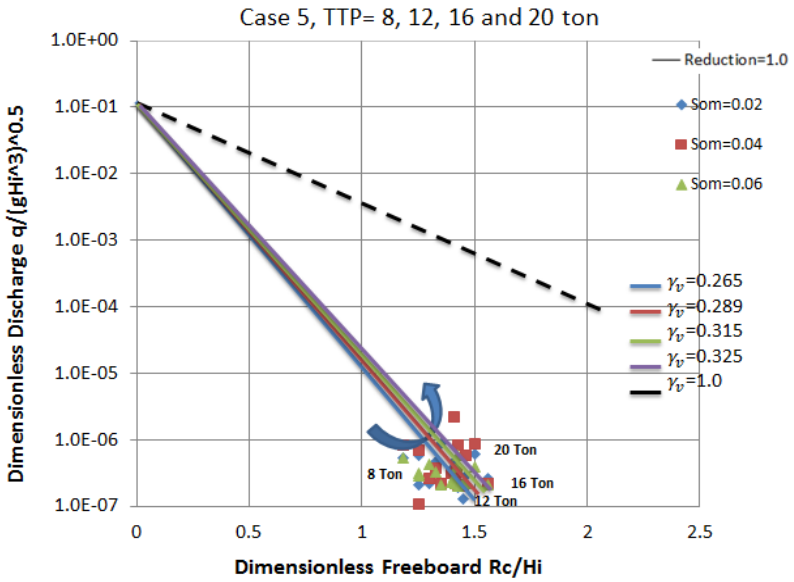

Fig. 20 Graph of non-dimensional mean overtopping versus the dimensionless freeboard for Case 5, TTP = 8 *ton*, 12 *ton*, 16 *ton* and 20 *ton*. The dashed lines are for $\gamma_v = 1.0$.

In total, a combination of 4 different tetrapod sizes (8 *ton*, 12 *ton*, 16 *ton* and 20 *ton*) and 4 different vertical wall heights were examined. Table 11 lists the test configuration used in this study. As tabulated in Table 11, a taller vertical wall can effectively reduce the overtopping discharge of the rubble mound. Similarly, a large tetrapod size decreases the overtopping discharge significantly. On the other hand, the unique point found in this study was that the height of the vertical wall can be reduced in the presence of a large tetrapod size. This finding is in a good agreement with the results reported by Van deer Meer (2002), in which for $R_c = A_c$ a roughness factor of 0.38 was suggested.

Table 11 Final γ_v values for a 1:2 sloping structure.

Case number	Vertical wall height (cm)	Influence factor for a vertical wall (γ_v)				Influence factor for roughness (γ_f)			
		TTP=8				TTP=12			
Case 1	0	1	1	TTP=16	TTP=20	TTP=8	TTP=12	TTP=16	TTP=20
Case 2	1.78	0.87	0.892	1	1	0.354	0.348	0.345	0.328
Case 3	3.53	0.368	0.375	0.902	0.917	Const.	Const.	Const.	Const.
Case 4	6.83	0.302	0.335	0.386	0.388	Const.	Const.	Const.	Const.
Case 5	9.33	0.265	0.289	0.347	0.363	Const.	Const.	Const.	Const.

Fig. 21 summarizes the variation in vertical wall factor against the roughness factor for all successful experiments in this study.

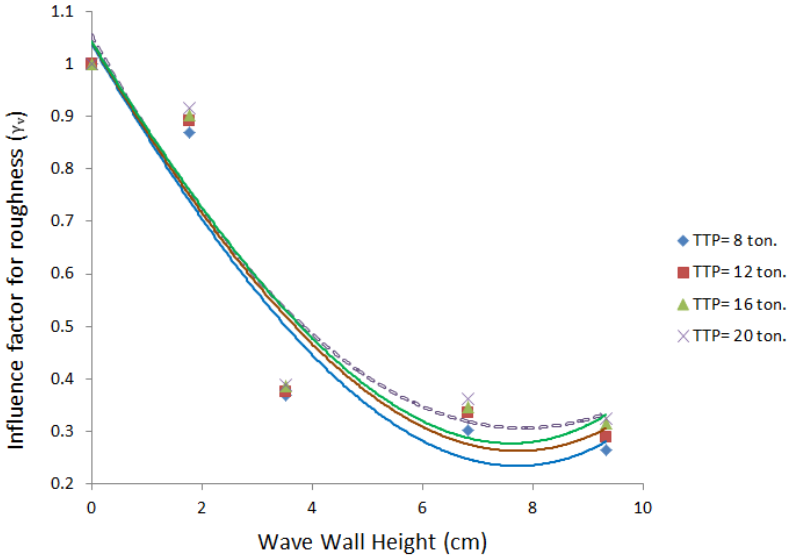

Fig. 21 Graph of non-dimensional mean overtopping versus dimensionless freeboard for Cases 1, 2, 3, 4, and 5, TTP = 8 *ton*, 12 *ton*, 16 *ton* and 20 *ton*, Dashed lines are for $\gamma_v = 1.0$.

CONCLUSION

The results of the physical model overtopping tests, which were carried out as a part of the project in Busan Yacht Harbor, were used to analyze the effects on different sizes of armor layer tetrapods along with the variation of the vertical wall height. Initially, the experiment was performed to observe how the overtopping discharge is affected by a variety of factors, such as wave steepness, significant wave height, and geometric characteristics of rubble mound structures. Thereafter, the effect of the vertical wall height and tetrapod size on the overtopping discharge in the rubble mound structure was investigated. In the presence of no vertical wall or a short one, the tetrapod size plays a key role in the overtopping discharge. In such circumstances, the overtopping discharge decreases with increasing tetrapod size. In the presence of medium and tall vertical walls, both the vertical wall factor and roughness factor mutually affect the overtopping discharge. In such a case, the general trend is that the value of the overtopping discharge decreases with increasing vertical wall height.

ACKNOWLEDGEMENTS

This study was supported by BK21 PLUS Program for Leading Universities and Students of Pusan National University.

REFERENCES

Aminti, P.L. and Frranco, L., 1988. Wave overtopping on rubble mound breakwaters. *Proceedings 21st International Conference on Coastal Engineering, ASCE,* Malaga, Spain, June 1988, pp.770-781.

Bradbury, A.P. and Allsop, N.W.H., 1988. Hydraulic effects of breakwater crownwalls. *Proceedings Conference on Design of Breakwaters,* Institution of Civil Engineers, Thomas Telford, London, May 1988, pp.385-396.

Bruce, T., van der Meer, J.W., Franco, L. and Pearson, L.M., 2009. Overtopping performance of different armour units for rubble mound breakwaters. *Special Issue of Journal of Coastal Engineering*, 56(2), 2009, pp.166-179.

Busan Port Authority, 2011. World port of source, Port of Busan. [online] Avaliable at: <http://www.worldportsource.com> [Accessed July 2011].

Franco, L., de Gerloni, M. and van der Meer, J.W., 1994. Wave overtopping at vertical and composite breakwaters. *ASCE, Proceedings of 24th International Conference on Coastal Engineering*, Kobe, Japan, 23-28 October 1994, pp.1030-1045.

Franco, L., 1993. Overtopping of vertical face breakwaters, results of model tests and admissible overtopping rates. *Proceedings MAST2-MCS, 1st project workshop*, Madrid, Spain, October 1993.

Franco L., Geeraerts J., Briganti R., Willems M., Bellotti G. and J. De Rouck., 2009. "Prototype and small-scale model tests of wave overtopping at shallow rubble-mound breakwaters" the Ostia-Rome yacht harbour case. Coastal Engineering, 56, pp.154-165.

Goda, Y., 1985. *Random seas and design of maritime structures*. Tokyo: University of Tokyo Press.

Jensen, O.J. and Juhl, J., 1987. Wave overtopping on breakwaters and sea dikes. *Proceedings of Second international conference on coastal and port engineering in developing countries*, Beijing, China, September 1987.

Mansard, E.P.D. and Funke, E.R., 1980. Measurement of incident and reflected spectra using a least squares method. *National Conference Publication Institution of Engineers,* Sydney, Australia, 1980, pp.154-172.

Owen, M.W., 1980. *Design of seawalls allowing for wave overtopping*. Wallingford: Hydraulics Research Station.

Pullen, T., Allsop, N.W.H., Bruce. T., Kortenhaus, A., Schuttrumpf, A. and Van der Meer, J.W., 2007. *EurOtop - wave overtopping of sea defences and related structures: ASSESSMENT manual*. Hamburg: Die Kuste.

Saville, T. and Caldwell, J.M., 1953. Experimental study of wave overtopping on shore structures. *Proc. of Minnesota International Hydraulics Convention*, IAHR, ASCE, Minneapolis, Minnesota, USA, May, 1953. pp. 261-269.

Van der Meer, J.W., 2002. Technical report on wave run-up and wave overtopping at dikes. *Technical Advisory Committee on Flood Defence*. Delft, The Netherlands, May 2002.

Van der Meer, J.W. and De Waal, J.P., 1993. *Water movement on slopes. Influence of berm, roughness, shallow foreshore and oblique long- and short- crested wave attack.* Delft: Delft Hydraulics.

Weggel, R.J., 1976. Wave overtopping equation. *Fifteenth Coastal Engineering Conference*, American Society of Civil Engineers, New York, USA, July 1976, pp.2737-2755.